available at www.sciencedirect.com

ScienceDirect

journal homepage: www.elsevier.com/locate/modo

MECHANISMS OF DEVELOPMENT

Localization of RhoGEF2 during *Drosophila* cellularization is developmentally controlled by *slam*

Christian Wenzl [a,*], *Shuling Yan* [a], *Philip Laupsien* [a,b], *Jörg Großhans* [a]

[a] *Institut für Biochemie und Molekulare Zellbiologie, Georg-August-Universität Göttingen, Justus-von-Liebig-Weg 11, 37077 Göttingen, Germany*

[b] *Center of Excellence – Cellular Networks, Universität Heidelberg, Im Neuenheimer Feld 282, 69120 Heidelberg, Germany*

ARTICLE INFO

Article history:
Received 23 December 2009
Accepted 4 January 2010
Available online 11 January 2010

Keywords:
Rho signalling
RhoGEF2
Drosophila
Cellularization
Developmental control

ABSTRACT

Essential for proper function of small GTPases of the Rho family, which control many aspects of cytoskeletal and membrane dynamics, is their temporal and spatial control by activating GDP exchange factors (GEFs) and deactivating GTPase-activating-proteins (GAPs). The regulatory mechanisms controlling these factors are not well understood, especially during development, when the organization and behaviour of cells change in a stage dependent manner. During *Drosophila* cellularization Rho signalling and RhoGEF2 are involved in furrow canal formation and the organization of actin and myosin. Here we analyze, how RhoGEF2 is localized at the sites of membrane invagination. We show that the PDZ domain is necessary for localization and function of RhoGEF2 and identify Slam as a factor that is necessary for RhoGEF2 localization. We also demonstrate that Slam can recruit RhoGEF2 to ectopic sites. Furthermore we find that the PDZ domain of RhoGEF2 can form a complex with Slam *in vivo* and that Slam transcripts and protein colocalize at the furrow canal and in basal particles. Based on these findings, we propose that accumulation of *slam* mRNA and protein at the presumptive invagination site provides a spatial and temporal trigger for RhoGEF2-Rho1 signalling.

1. Introduction

RhoGTPases regulate many aspects of the actin cytoskeleton and membrane organization and thus control cell polarity, behaviour, morphology and division (Jaffe and Hall, 2005). Switching between an inactive GDP-bound and an active GTP-bound conformation, Rho proteins activate effector enzymes like protein kinases, formins and other cytoskeletal regulators as well as different scaffold proteins (Bustelo et al., 2007). Important for the cellular organization and behaviour is the spatial and temporal control of Rho activation, which is achieved by a balance of GEF and GAP enzymes at selected membrane domains (Schmidt and Hall, 2002a; Tcherkezian and Lamarche-Vane, 2007).

Although it is clear that Rho activation is spatially and temporally regulated, the exact molecular mechanisms that underlie this tight control are not well defined. A prominent example of locally regulated Rho activation is cytokinesis of animal cells (D'Avino et al., 2005). Here the separation of the two newly formed daughter cells is achieved by the assembly of a contractile ring in the cleavage plane of the mother cell followed by constriction and subsequent scission. The activity of a Rac specific GAP, which is a component of the centralspindlin complex as well as the activity of the RhoGEF Ect2/Pebble are required to form a narrow zone of Rho activation at the overlaying cell cortex. Rho activation is a prerequisite for the assembly of the actomyosin filaments that drive constriction (Bement et al., 2005; Kamijo et al., 2006; Lee et al., 2004; Somers and Saint,

* *Corresponding author.* Tel.: +49 551 398242.
E-mail address: cwenzl@gwdg.de (C. Wenzl).
0925-4773/$ - see front matter
doi:10.1016/j.mod.2010.01.001

2003; Tatsumoto et al., 1999). In addition to the spatial control of Rho activity, the temporal regulation is equally essential, especially during development. During the epithelial to mesenchymal transition (EMT) in avian gastrulation, RhoA is localized basally in pre-EMT epiblast cells by the RhoGEF Net1 (Nakaya et al., 2008). One suggested mechanism to regulate Rho activity in the cytoplasm is the nuclear sequestration and signal dependent cytoplasmic release of GEFs like Pebble and Net1 (Prokopenko et al., 1999; Schmidt and Hall, 2002b). However, this type of regulation cannot account for the control of the polarized localization of GEFs and their restricted activation at membrane domains. This means that additional mechanisms assure the proper spatial and temporal control of GEF activity.

Drosophila cellularization offers an excellent system to study Rho activation in a developmental context. Early embryonic development of *Drosophila* starts with a series of 13 rapid nuclear divisions that proceed in a common cytoplasm without cytokinesis. After 13 divisions the cell cycle pauses and during interphase of cell cycle 14 the somatic nuclei of the syncytial blastoderm that are arranged as a cortical monolayer are enclosed into cells by invagination of the plasma membrane in a process called cellularization (Mazumdar and Mazumdar, 2002). At the onset of interphase 14 similar as in previous interphases filamentous actin forms caps at the cortex apically to the nuclei. Within the next few minutes f-actin is reorganized and gradually accumulates at the tip of the invaginating membrane, the furrow canal (Schejter and Wieschaus, 1993; Warn and Magrath, 1983). This reorganization of the actin cytoskeleton depends on Rho1. Inhibition of Rho1 function by drugs or expression of dominant-negative alleles leads to a disruption of the actin cytoskeleton and to severe defects during membrane invagination (Crawford et al., 1998). We and others have described previously the functions of RhoGEF2 and the Rho1 effector Dia during blastoderm formation of *Drosophila* embryos (Afshar et al., 2000; Grosshans et al., 2005; Padash Barmchi et al., 2005). In *RhoGEF2* mutants the furrow canals are often incorrectly formed and sometimes missing. Rho1 fails to localize to the furrow canal and the levels of furrow canal associated f-actin are reduced. RhoGEF2 is a large multidomain protein with homology to the mammalian LARG and with multiple developmental functions. Beside its role in cellularization, *RhoGEF2* is involved in apical constriction of cells that precedes mesoderm invagination during *Drosophila* gastrulation when it receives input from the small G protein Concertina (Barrett et al., 1997; Häcker and Perrimon, 1998; Kölsch et al., 2007). Furthermore, it was shown to be involved in the formation of segmental grooves during mid-embryogenesis (Mulinari et al., 2008) as well as in epithelial invagination during salivary gland formation and in the formation of a proper wing epithelium (Nikolaidou and Barrett, 2004). So far different models have been proposed to explain how RhoGEF2 and thus Rho activation is targeted to specific membrane compartments. One is based on the observation that GFP-RhoGEF2 is dynamically associated with microtubule plus ends in S2 cells in an EB1 dependent manner and that this association can be released by the activated form of the Gα subunit Concertina. It has been suggested that this mechanism might be involved in the RhoGEF2 mediated apical constriction of presumptive mesoderm cells (Rogers et al., 2004). Targeting proteins to certain membrane domains by MT plus end mediated transport has been reported in other systems (Shaw et al., 2007), however, the physiological significance of the MT plus end localization has not yet been confirmed in a living organism. A second model suggests that a recycling endosome dependent vesicle transport mechanism contributes to the localization of RhoGEF2 to metaphase furrows during syncytial divisions. This is based on studies that showed that localization of RhoGEF2 to metaphase furrows is disturbed in *nuf* and *Rab11* embryos (Cao et al., 2008). Here we show that the localization of RhoGEF2 at the furrow canal is required for the protein function during cellularization. We identified the PDZ domain of RhoGEF2 as the domain necessary and sufficient for furrow canal localization. Furthermore, we present evidence that the localization of RhoGEF2 at the furrow canal is controlled by Slam. Interestingly *slam* belongs to a group of early zygotic genes whose expression peaks during cellularization. Slam is required for timely invagination of the membrane furrows (Lecuit et al., 2002; Stein et al., 2002). Besides a functional relation, we also show that Slam can interact with the PDZ domain of RhoGEF2 *in vivo*. Finally, we show that *slam* mRNA shows a unique furrow canal localization suggesting a mechanism, where the polarized membrane localization of *slam* transcripts mediates RhoGEF2 localization, which in turn controls Rho activity during furrow canal formation.

2. Results

2.1. The PDZ domain targets RhoGEF2 to the furrow canal

We and others have previously reported that RhoGEF2 contributes to the assembly of actin–myosin at the furrow canal by Rho1 mediated activation of the formin Dia, which is necessary to keep the proper morphology of the furrow canal (Grosshans et al., 2005; Padash Barmchi et al., 2005). To analyze how RhoGEF2 is targeted to the site of membrane invagination, we established an mRNA microinjection assay with myc-tagged constructs for testing RhoGEF2 localization (Fig. 1A). mRNA encoding full-length RhoGEF2 was injected into embryos from *RhoGEF2* germline clones (Fig. 1B). Since the full-length construct localized to the furrow canal as marked by co-staining for f-actin (Fig. 1B′), this assay can be employed for mapping the localization element. In a second step four constructs spanning the coding sequence of *RhoGEF2* were injected (Fig. 1A). All four constructs showed differential localization (Fig. 1C–F), only the N-terminal construct myc-RG2-1 accumulated in a pattern resembling full-length protein localization (Fig. 1C). We then used two constructs spanning the sequence of the construct myc-RG2-1 that were designed with a partial overlap containing the PDZ domain (data not shown). Since both constructs showed a similar furrow canal localization we concluded that the PDZ domain might be sufficient for mediating this localization. To confirm this hypothesis, we tested a construct encoding only the PDZ domain fused to the myc_6 tag. This protein of about 28 kDa could be detected mainly in the nucleus (data not shown). To circumvent the nuclear accumulation, we added more copies of the PDZ domain thereby increasing the molecular weight of the resulting fusion protein. This also increased the affinity for the furrow canal binding sites, since we observed a reduction

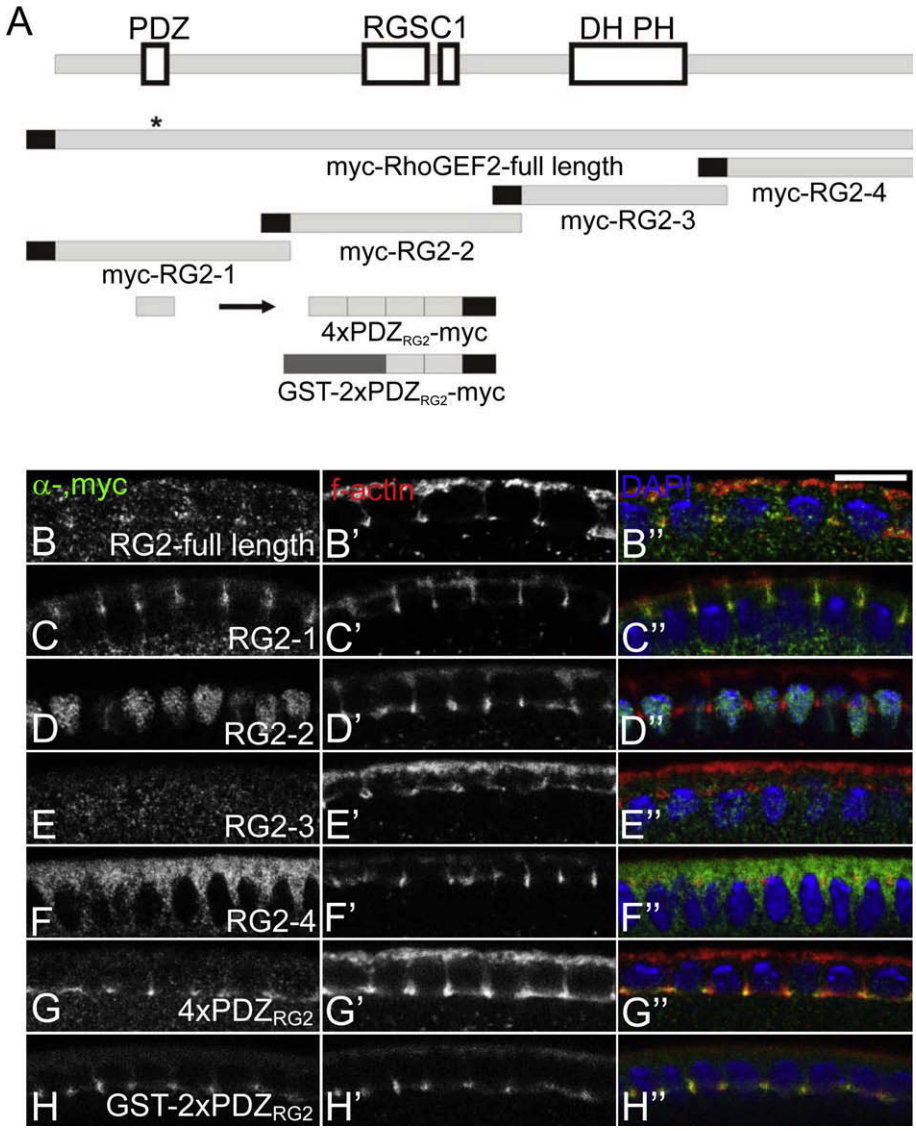

Fig. 1 – The PDZ domain of RhoGEF2 is sufficient for furrow canal localization. Fixed and stained embryos from *RhoGEF2*$^{l(2)04291}$ germline clones that were injected with mRNA encoding epitope-tagged fragments of RhoGEF2. (A) Schematic drawing of RhoGEF2 with structural domains and constructs tested in the injection assay. The asterisks marks the position of the amino acids substituted in myc-RhoGEF2(GAGA) (B–H) myc-staining, (B′–H′) phalloidin staining, (B″–H″) merge, DNA staining. Scale bar: 10 μm.

in cytoplasmatically localized protein. All tested constructs containing 2 or 4 copies of the PDZ domain fused to myc$_6$ could be detected at the furrow canal (Fig. 1G and H), thus confirming that the PDZ domain is sufficient for furrow canal localization. To test the influence of different protein tags, we injected mRNA encoding a GST-2xPDZ$_{RG2}$-myc$_6$ construct (Fig. 1H). Moreover we tested the localization dynamics *in vivo* by using a fly strain that expressed a *UAS-4xPDZ$_{RG2}$-RFP* transgene driven by a maternal *Gal4* driver (*Supplementary* Fig. S1A–D). Both constructs showed the expected furrow canal localization. To test whether the PDZ domain is also required for localization of full-length RhoGEF2, two amino acid residues of the carboxylate loop of the PDZ domain were mutated to generate myc$_6$-RhoGEF2(GAGA) (Fig. 2A). These residues are essential for ligand binding in the PDZ domain of the rat protein rPDZRhoGEF (Longhurst et al., 2006). This construct was expressed under the control of the ubiquitously active spagetti-squash promoter in germline clones of a *RhoGEF2* null allele (*RhoGEF2*^{04291}). Since the mutated protein was not enriched at the furrow canal (Fig. 2C and G), the PDZ domain is indeed required for localization of RhoGEF2. Moreover the PDZ domain is required for RhoGEF2 function, since in contrast to a respective wildtype construct (Fig. 2E and I), the myc$_6$-RhoGEF2(GAGA) transgene does not restore the furrow array during cellularization and thus does not complement the mutant phenotype (Fig. 2G and K). Moreover myc-RhoGEF2-T1544A, a *RhoGEF2* allele with a point mutation in the guanyl-nucleotide exchange domain (Grosshans et al., 2005), localized correctly but did not complement the *RhoGEF2* phenotype (Fig. 2F and J). This experiment shows that the multidomain protein RhoGEF2 indeed requires the Rho1 specific GEF activity for its function during cellularization.

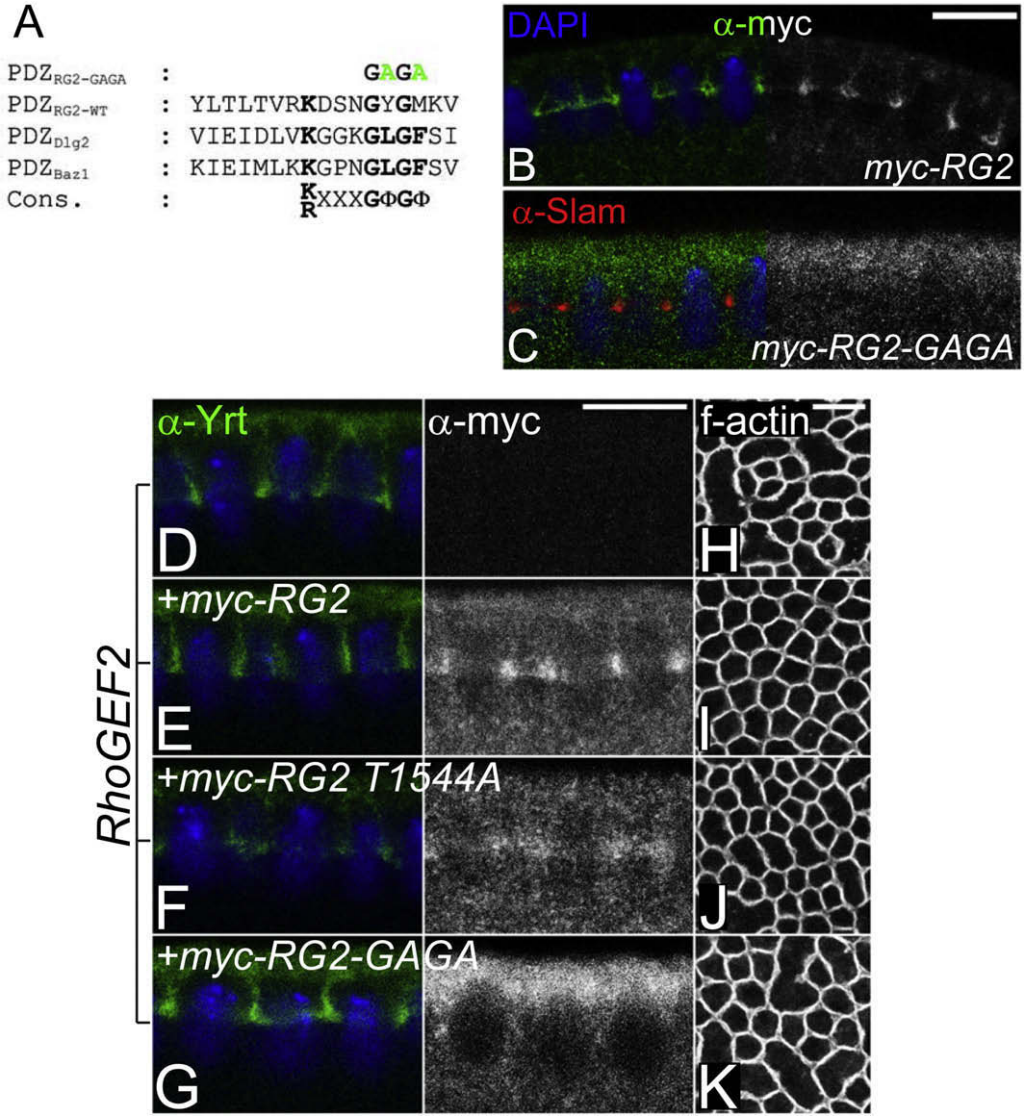

Fig. 2 – The PDZ domain is required for RhoGEF2 localization and function during cellularization. (A) Alignment of the amino acid sequences covering the conserved carboxylate binding loops of the PDZ domains of RhoGEF2 ($PDZ_{RG\text{-}WT}$), the second PDZ domain of Dlg (PDZ_{Dlg2}) and the first PDZ of Bazooka (PDZ_{Baz1}). The consensus sequence is given in the bottom line (X-unspecified, Φ-hydrophobic). Top line: two residues in the PDZ domain of RhoGEF2 (green) were substituted to generate myc-RhoGEF2(GAGA). (B and C) Embryos from transgenic flies expressing either *myc-RhoGEF2* (B) or *myc-RhoGEF2(GAGA)* (C) in wildtype background were stained for myc-tag or the furrow canal marker Slam. myc-RhoGEF2 localization is indistinguishable from endogenous RhoGEF2 (J, Grosshans et al., 2005). (D–G) The localization of the different myc-RhoGEF2 alleles was tested by staining for myc. The furrow canal is marked by α-Yrt staining (Laprise et al., 2006). No myc-signal is detected in RhoGEF2 embryos (D) whereas myc-RhoGEF2 and myc-RhoGEF2(T1544A) both localize at the furrow canal (E and F). In contrast myc-RhoGEF2(GAGA) does not localize to the furrow canal (G). (H–K) Myc-tagged RhoGEF2 constructs were expressed as transgenes in a RhoGEF2 amorphic background. The embryos shown are not the same embryos as in D–G. The presence of multinuclear cells in cellularizing embryos was scored to analyze the rescue activity of theses alleles. Embryos were fixed and stained for f-actin. In RhoGEF2 embryos multinuclear cells are present in 100% of counted embryos (H, $n = 52$). Expression of myc-RhoGEF2 fully complements this phenotype (I, $n = 25$), whereas expression of myc-RhoGEF2(T1544A) (J, $n = 35$) and myc-RhoGEF2(GAGA) (K, $n = 15$) did not. Scale bars: 10 μm.

2.2. *Slam is required for RhoGEF2 localization at the furrow canal*

PDZ domains are involved in assembling membrane associated signalling complexes by mediating protein–protein interactions (Jelen et al., 2003). To find factors that could be responsible for the PDZ-mediated furrow canal localization of RhoGEF2, we reinvestigated the role of Slam, a protein that is required for germ cell migration and for timely invagination of the plasma membrane during cellularization. The *slam* gene is characterized by a burst of expression exclusively at the onset of cellularization (Lecuit et al., 2002; Stein et al.,

2002). *Slam* mutant embryos showed strongly reduced RhoGEF2 staining at the furrow canal in direct comparison to their heterozygous or wildtype siblings (Fig. 3A and B), whereas levels of the lateral furrow marker Neurotactin (Nrt) remained relatively unaffected (Fig. 3C). We obtained similar results after staining for the lateral furrow marker Dlg, since the levels of Dlg and its localization to the lateral membrane were comparable in wildtype and in *slam* embryos (*Supplementary* Fig. S2A–J). Consistent with previous reports (Lecuit et al., 2002), Nrt was apically enriched in *slam* mutants (Fig. 3C; white arrowhead). The residual RhoGEF2 levels that were detectable in *slam* embryos may be due to the low maternal contribution of *slam* or to a redundant ligand. Testing the reverse relationship, we found that Slam localized normally in embryos from RhoGEF2 germline clones (Fig. 6N). The functional dependance of RhoGEF2 on Slam appears to be dose-dependent, since embryos with a Slam gradient along the anterior–posterior axis that was induced by posterior injection of *slam* dsRNA showed a corresponding RhoGEF2 gradient (Fig. 3E and F). Since other proteins such as Myosin II and Patj that are localized at the furrow canal were also dependent on *slam* (Fig. 3G; *Supplementary* Fig. S3H and K), two possibilities are conceivable to explain the observed functional relation between RhoGEF2 and Slam. One explanation could be that furrow canal localization of RhoGEF2 depends specifically on Slam due to a direct or indirect protein interaction. Alternatively the furrow canal is simply absent or dysfunctional, which would result in a non-specific loss of all furrow canal markers. To further analyze the link of Slam and RhoGEF2 we tested RhoGEF2 localization in germline clones of $slam^{waldo1}$, a *slam* allele with a premature stop codon (Stein et al., 2002). The levels and the prominent accumulation of the truncated Slam protein at the furrow canal were lower than in wildtype embryos (*Supplementary* Fig. S3A, D, G and J). RhoGEF2 enrichment at the furrow canal was strongly reduced, while Patj staining was almost absent (*Supplementary* Fig. S3B, E, H and K), indicating that Slam differentially controls furrow canal localization of RhoGEF2 and Patj.

2.3. *Slam and PDZ_{RG2} interact biochemically*

One possible mechanism that could explain the observed functional relation between RhoGEF2 and Slam is that RhoGEF2 gets recruited to the furrow canal by a physical interaction with Slam. To test this hypothesis, we isolated Slam complexes by immunoprecipitation from staged embryos. We raised an antibody against Slam and tested this antibody for specificity in Western blots (Fig. 4A). A band at an apparent molecular weight of above 175 kDa could be detected, which is higher than the predicted molecular weight of 130 kDa. Nevertheless in extracts from embryos expressing a GFP-Slam fusion protein a second band with an apparent higher molecular weight is detected in addition to the 175 kDa band. This band can also be detected by using an anti-GFP antibody. $Slam^{waldo1}$ was reported to contain a premature stop codon, which should result in a truncated protein with a predicted size of about 80 kDa. In embryonic extracts from $slam^{waldo1}$ germline clones we could detect a second band of about 100 kDa in addition to the 175 kDa band of full-length Slam (Fig. 4B). The $slam^{waldo1}$ extract also contains full-length Slam protein, since zygotically homozygous and heterozygous embryos were not sorted. Taken together these results show that our antibody is specific for Slam. Since the full-length RhoGEF2 protein cannot be robustly detected in Western blots with embryonic extracts, we employed transgenic embryos expressing a $4xPDZ_{RG2}$-myc_6

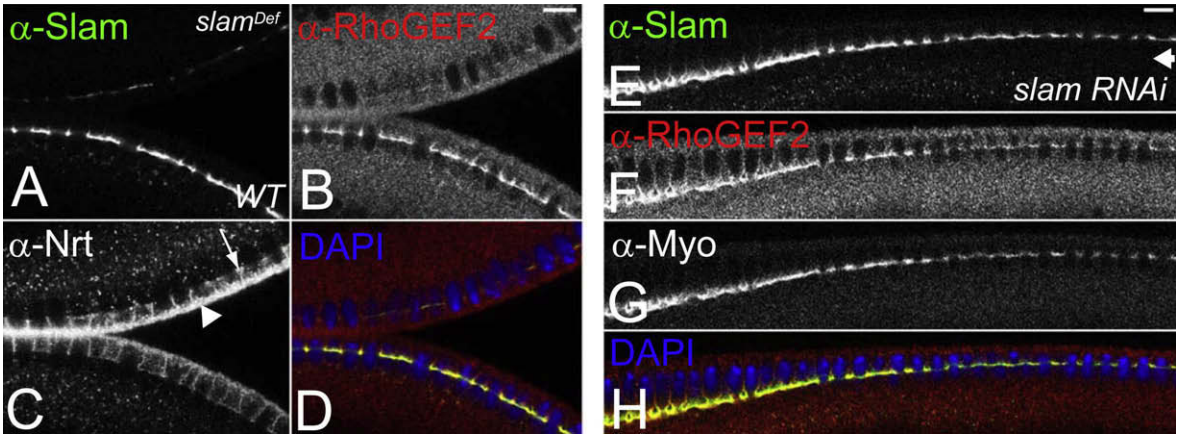

Fig. 3 – Furrow canal localization of RhoGEF2 depends on *slam* in a dose-dependent manner. Embryos from flies heterozygous deficient for *slam* were stained for Slam (A), RhoGEF2 (B) and Neurotactin (Nrt, C), (D) merge and DNA stain. Zygotically homozygous embryos are marked by low levels of Slam staining and the characteristic mutant morphology. The weak Slam staining in the mutant represents the maternal Slam contribution. The levels of RhoGEF2 at the furrow canal are strongly reduced in $slam^{Def}$ embryos (B), whereas the levels of Nrt are less affected (C). Note the apical enrichment (white arrowhead) and the unusual accumulation of Nrt at the furrow canal (white arrow) in *slam* embryos. (E–H) A wildtype embryo posteriorly injected with dsRNA specific for *slam* was stained for Slam (E), RhoGEF2 (F) and Myosin II (G). (H) Merge and DNA stain. The white arrow marks the posterior injection site. Notice the gradient of protein levels and *slam* function (as seen by the invagination depth of the membrane front) towards the injection site. The levels of RhoGEF2 and Myosin II are gradually reduced to a similar extent. Scale bar: 10 μm.

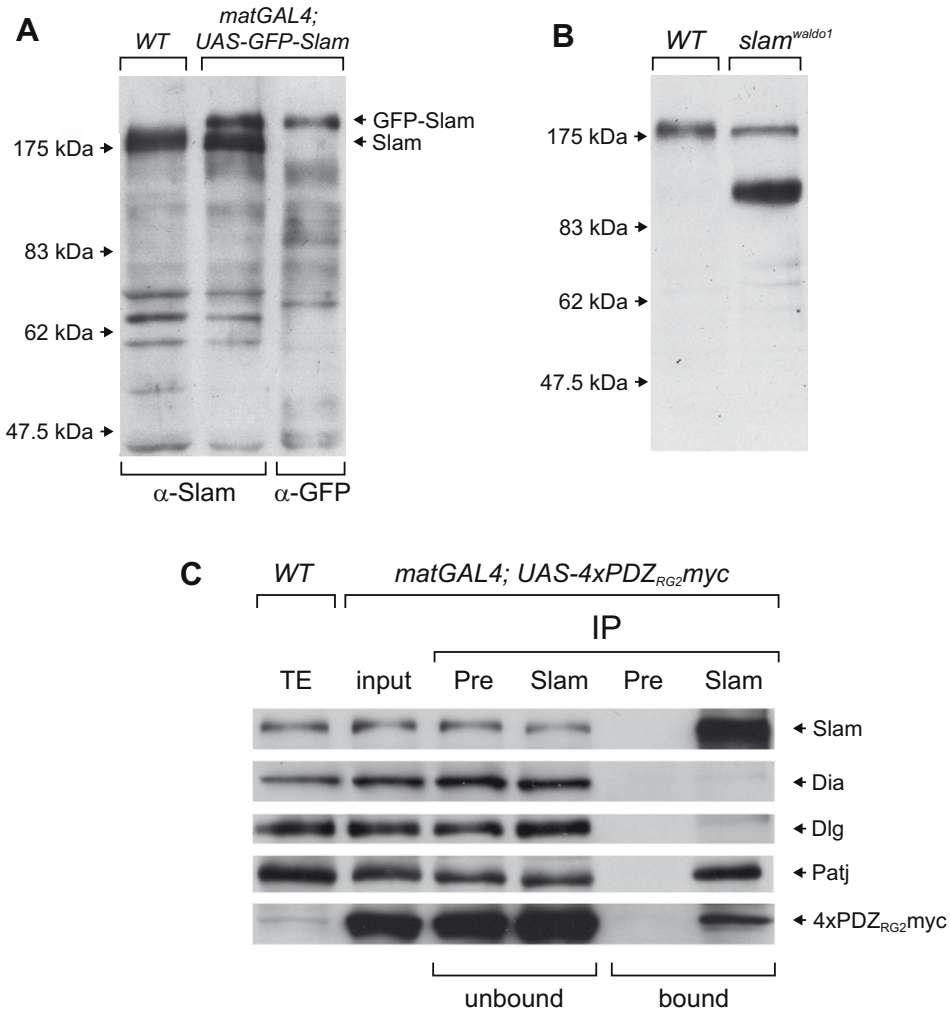

Fig. 4 – The PDZ domain of RhoGEF2 can physically interact with Slam *in vivo*. (A and B) Western blots showing the specificity of the Slam antibody. In extracts from wildtype embryos a single band (~175 kDa) in extracts from GFP-Slam expressing embryos two bands (~175 and ~200 kDa) are detected (A, left and middle lane). The band at ~200 kDa is also detected by a GFP antibody (A, right lane). (B) In embryonic extracts from wildtype embryos (B, left lane) and from *slam*^{waldo1} germline clones (B, right lane) a 175 kDa is detected. In *slam*^{waldo1} extracts a second band with a molecular weight of about 100 kDa is present which probably corresponds to the C-terminally truncated Slam^{waldo1} protein. All Slam proteins run at significantly higher molecular weights than predicted. (C) Western blots of co-immunopreciptations from embryonic extracts using preimmune serum (Pre) and Slam antibody were probed with α-Slam, α-Dia, α-Dlg, α-Patj and α-myc antibodies. TE: total extract from wildtype embryos (first lane), input: sample of the extract of 4xPDZ$_{RG2}$-myc$_6$ expressing embryos (second lane), unbound: supernatant samples after IP (lanes 3 and 4), bound: samples of proteins eluted from beads after IP (lanes 5 and 6). Whereas Slam, Patj and 4xPDZ$_{RG2}$-myc$_6$ do co-immunoprecipitate using the Slam-antibody, Dia and Dlg do not (last lane). In the co-IP performed using the preimmune serum a weak association of 4xPDZ$_{RG2}$-myc$_6$ was detected (lane 5). The sample volume loaded in lane 1–4 corresponds to ~10 embryos, in lanes 5 and 6 to ~500 embryos.

fusion protein for immunoprecipitation experiments (Fig. 4C). This fusion protein showed a more exclusive localization at the furrow canal than the full-length RhoGEF2 protein (Fig. 1B and G). Slam protein was enriched in the bound fraction. We found that the PDZ construct and Patj, which like RhoGEF2 depends on Slam for its localization, were enriched in the bound fraction. Other proteins like Dia and Dlg fully remained in the unbound fraction. This experiment shows that Slam, Patj and 4xPDZ$_{RG2}$-myc$_6$ are part of the same biochemical complex in the tested embryos. Given that 4xPDZ$_{RG2}$-RFP localizes similarly as RFP-RhoGEF2 (*Supplementary* Fig. S1) the IP-experiments are consistent with the hypothesis that RhoGEF2 and Slam physically interact in the embryo. Although we were not able to demonstrate an interaction of full-length RhoGEF2 and Slam, our data suggest that Slam could control RhoGEF2 localization by a direct or indirect interaction with the PDZ domain of RhoGEF2.

2.4. *Slam can recruit RhoGEF2 to ectopic sites*

Since Slam can form a complex with the PDZ domain of RhoGEF2 *in vivo*, we wondered whether Slam could recruit

RhoGEF2 to ectopic sites. First we locally injected mRNA encoding a myc-tagged Slam construct into wildtype embryos to increase the Slam levels (Fig. 5A–C). Correspondingly the staining levels for endogenous RhoGEF2 at the furrow canal

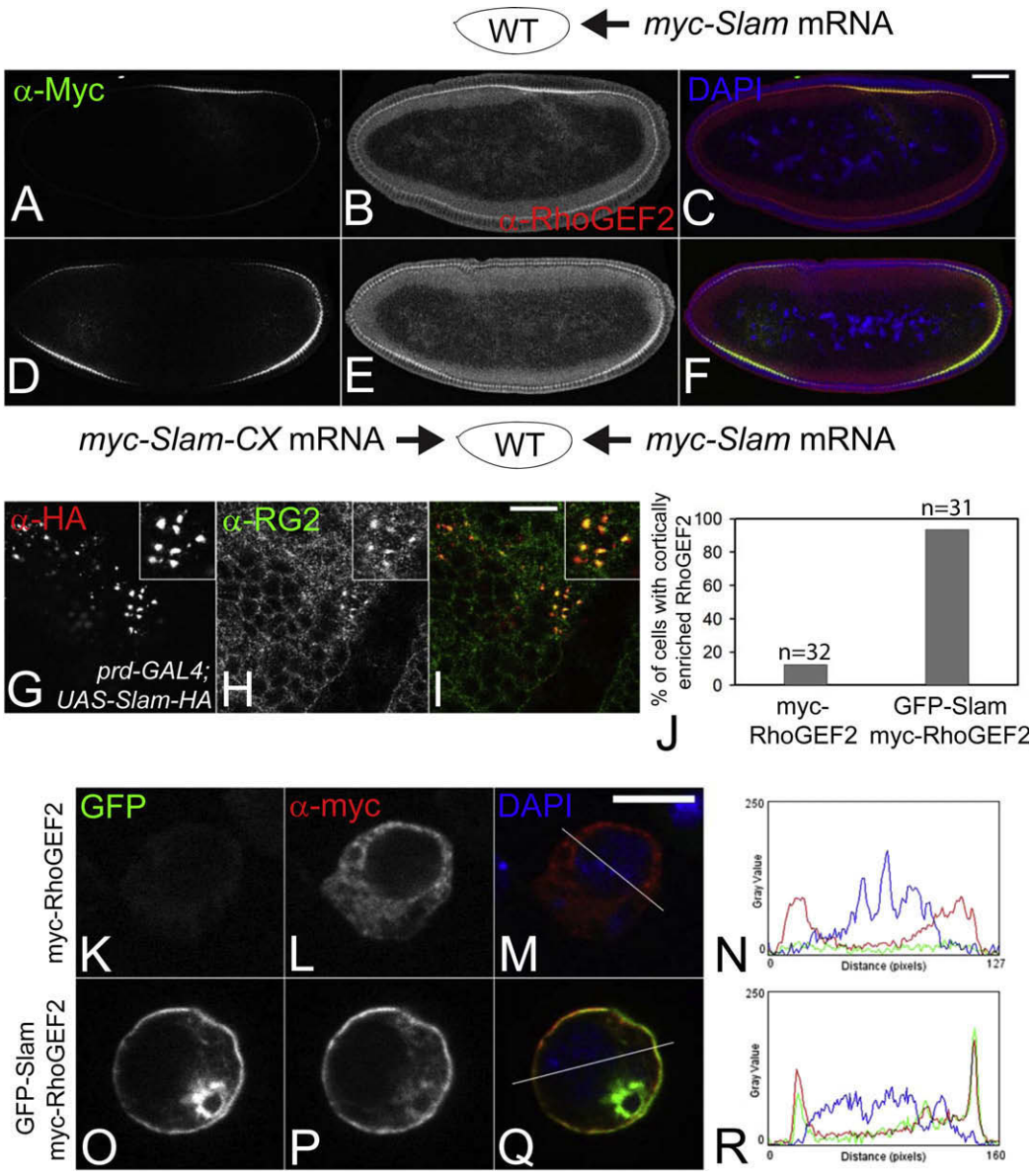

Fig. 5 – Slam can recruit RhoGEF2 to ectopic sites. (A–F) WT embryos injected with mRNAs encoding indicated myc-Slam constructs were stained for α-myc (A and D) and α-RhoGEF2 (B and E). (C and F) Merge and DNA stain. (A–C) Posterior injection of myc-Slam. Elevated myc-staining can be observed close to the injection site (dorsal part in A). Correspondingly furrow canal levels of RhoGEF2 are also locally increased (B). The invagination in the injected dorsal area has further proceeded compared to the adjacent regions. (D–F) Posterior injection of myc-Slam and anterior injection of myc-Slam-CX (two point mutations in the putative C-terminal PDZ binding motive). Both Slam proteins localize to the furrow canal and form gradients with the highest protein levels close to the injection site (D). RhoGEF2 is gradually enriched at the furrow canal both in the anteriorly and the posteriorly injected region (E). Scale bar: 100 μm. (G–I) A Slam-HA fusion was ectopically expressed using the UAS/Gal4 system in seven *prd*-stripes in stage 7–9 embryos. Embryos were fixed and stained for HA (G) and RhoGEF2 (H). Slam-HA is enriched in large punctuate structures at the basal end of epithelial cells (G). RhoGEF2 is also enriched in these structures within the Slam-HA expression domains but cannot be detected in similar structures in regions without Slam-HA expression (H). (I) Merge. K-R: *Drosophila* S2 cells were transiently transfected either with myc-RhoGEF2 (K–N) or with GFP-Slam and myc-RhoGEF2 (O–R). Cells were fixed and stained for myc. Under the applied fixation conditions myc-RhoGEF2 is uniformly localized throughout the cytoplasm (L). Upon co-expression of GFP-Slam, which localizes to the cell cortex (O), myc-RhoGEF2 can be detected at the cell cortex (P). (N and R) The intensity profiles of the GFP, the myc and the DAPI signals were plotted along the white lines shown in (M) and (P). (J) Quantification of cortical enrichment of myc-RhoGEF2 in cells with and without GFP-Slam expression.

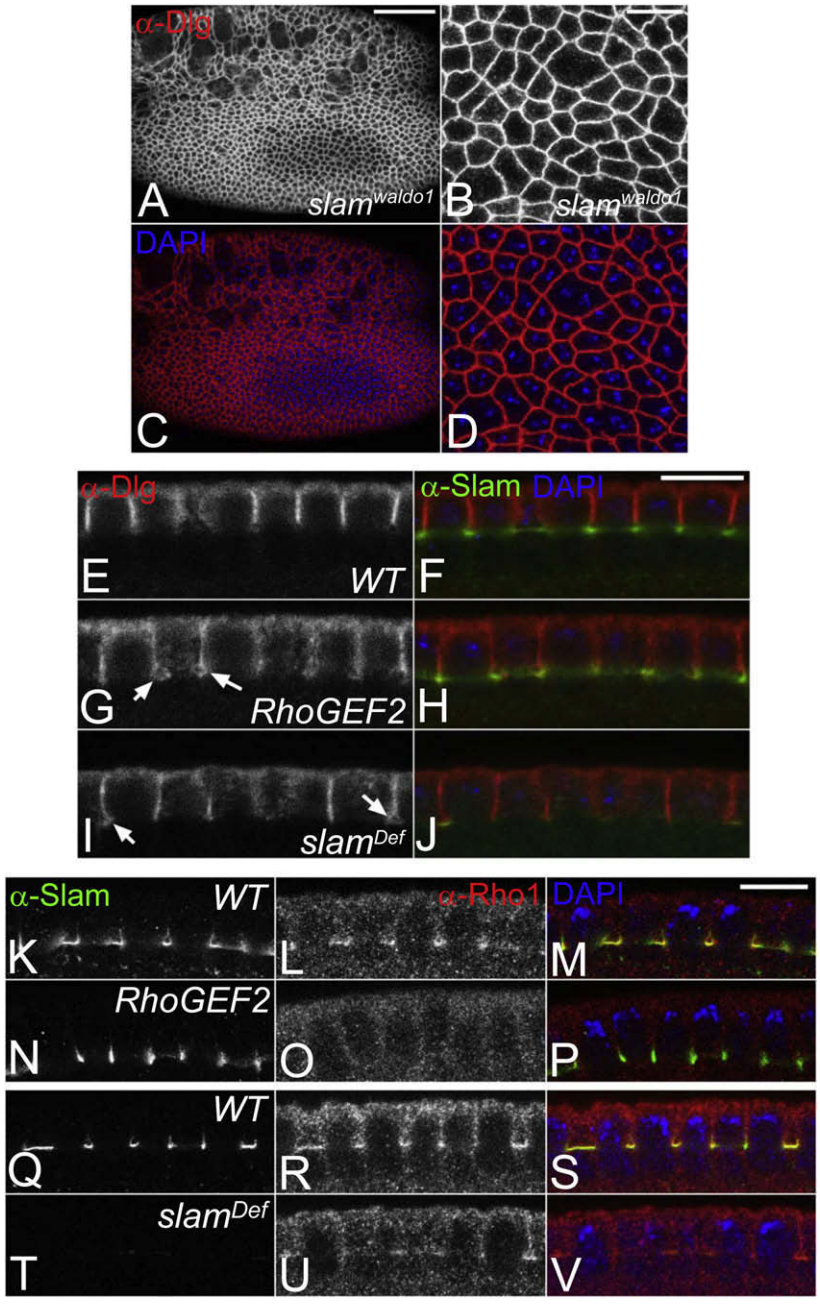

Fig. 6 – Specific aspects of the RhoGEF2 cellularization phenotype can be observed in *slam* mutant embryos. (A–D) Cellularizing embryos of $slam^{waldo1}$ germline clones were fixed and stained with α-Dlg antibody (A and B). (C and D) DNA stain and merge. Similar as in *RhoGEF2* mutant embryos the formation of the hexagonal array of invaginating membranes is disturbed leading to multinuclear cells which become visible especially in late cellularization. (E–J) The integrity of cortical compartments is disturbed in *RhoGEF2* as well as in *slam* mutant embryos. *WT*, *RhoGEF2* and $slam^{Def}$ embryos were fixed and stained with α-Slam and α-Dlg antibody. Whereas in *WT* the lateral marker Dlg and the furrow canal protein Slam localize to separate cortical compartments without significant overlap (E and F), Dlg can be detected in the furrow canal domain both in *RhoGEF2* (G white arrows) and in $slam^{Def}$ embryos (I, white arrows) where it overlaps with Slam (H and J). (K–V) The levels of Rho1 at the furrow canal are reduced in *slam* embryos. *WT*, *RhoGEF2* and $slam^{Def}$ embryos were fixed and stained for Slam (K, N, Q, T) and Rho1 (L, O, R, U). (M, P, S, V) Merge and DNA stain. Whereas in *WT* embryos Rho1 is enriched at the furrow canal (L and M) this localization cannot be detected in *RhoGEF2* embryos (O and P, consistent with Padash Barmchi et al., 2005). *WT* and *RhoGEF2* embryos were stained in the same tube. Staining of $slam^{Def}$ embryos revealed reduced levels of Rho1 at the furrow canal (U) compared to the staining in a heterozygous sibling (R). Rho1 localization is not completely abolished since low levels of RhoGEF2 remain associated with the furrow canal of *slam* embryos (see Fig. 2). Scale bar in (A): 100 μm, all other scale bars: 10 μm.

increased (Fig. 5B), what shows that Slam controls RhoGEF2 levels in a dosage dependent manner. This is consistent with the RhoGEF2 levels of embryos where Slam was gradually downregulated by dsRNA injection (Fig. 3E and F).

Proteins containing PDZ domains often interact with transmembrane proteins that contain a PDZ binding motif at their cytoplasmic tail (Jelen et al., 2003). Slam is a novel membrane associated protein (Lecuit et al., 2002) without any known functional domains. Nevertheless, it contains a potential class II PDZ binding motif at its C-terminus (-AVEV). Using our injection assay we directly compared the activity of a wildtype construct to a *slam* allele with a mutated C-terminus (-AAEA). The mRNA encoding the wildtype allele was injected at the posterior pole, the mRNA encoding the mutant allele, at the anterior pole (Fig. 5D–F). Staining of such embryos for RhoGEF2 shows that both *slam* alleles can equally recruit additional RhoGEF2 to the furrow canal (Fig. 5E). This suggests that the recruitment of RhoGEF2 by Slam does not occur via a conventional direct interaction between the PDZ of RhoGEF2 and the putative PDZ binding motif at the C-terminus of Slam.

To test whether Slam is sufficient for RhoGEF2 localization, we established a recruitment assay in cultured cells, which did not show any detectable *slam* expression. Under the fixation conditions used, both endogenous (data not shown) and transiently expressed myc-tagged RhoGEF2 are uniformly distributed in the cytoplasm with no obvious enrichment at the plasma membrane (Fig. 5L and N). Co-expression of GFP-Slam, which displayed a sharp peripheral distribution (Fig. 5O), lead to a corresponding peripheral enrichment of myc-RhoGEF2 protein (Fig. 5P and R) in the vast majority of the cells (Fig. 5J). This ectopic recruitment of RhoGEF2 was confirmed by expression of *slam* in the embryonic epidermis. Upon expression of a *UAS-Slam-HA* construct by a *prd-GAL4* driver in seven stripes of epidermal cells Slam-HA localizes to structures at the basal end of epidermal cells, whose nature and function are unknown (Fig. 5G–I). The cells between the stripes serve as a staining control. Co-staining for RhoGEF2 shows that there is a strong correlation of Slam and RhoGEF2 (Fig. 5H and I). Taken together these experiments show that ectopically localized Slam protein can either directly or indirectly recruit RhoGEF2 and that this recruitment does not depend on the C-terminus of Slam.

2.5. *Slam deficient embryos exhibit aspects of the RhoGEF2 phenotype*

If RhoGEF2 depends on Slam in functional terms, at least some aspects of the mutant phenotype of *RhoGEF2* will be visible in the *slam* mutants. In embryos from *RhoGEF2* germline clones, there are gaps in the furrow array that lead to the formation of multinuclear cells (Grosshans et al., 2005). Close examination of embryos from $slam^{waldo1}$ germline clones showed that indeed gaps in the furrow array are observed mostly in the ventral region (Fig. 6A–D). Although the gaps resemble the *RhoGEF2* mutant phenotype, such a regional bias is not observed in embryos from *RhoGEF2* germline clones.

Triggered by the recent report that *nullo* is required for separation of basal and lateral membrane markers (Sokac and Wieschaus, 2008b), we reexamined the *RhoGEF2* mutant phenotype. We found that similar as in *nullo* embryos, the lateral marker protein Dlg, which is normally excluded from the furrow canal and does not overlap with Patj, Slam or RhoGEF2 (Fig. 6E and F), extended into the furrow canal in embryos from *RhoGEF2* germline clones (Fig. 6G). In *slam* mutant embryos a similar distribution of Dlg was observed (Fig. 6I). Although these experiments do not show that these aspects of the *slam* mutant phenotype are caused by lacking RhoGEF2 function, they show that *slam* is involved in the same processes as *RhoGEF2*.

A third aspect of the phenotype of a *RhoGEF2* null mutant is that Rho1 does not localize at the furrow canal (Fig. 6O). This aspect of the phenotype is specific for *RhoGEF2* since Rho1 does localize normally in *nullo* mutants (data not shown). In contrast, we find that furrow canal levels of Rho1 are clearly reduced in *slam* mutants (Fig. 6R and U). The protein is not completely absent, since low levels of RhoGEF2 are present at the furrow canal in *slam* zygotic mutants. Taken together, these data suggest that specific aspects of the complex *slam* phenotype can be explained by the loss of the spatial control of Rho1 activity at the furrow canal, which might be based on a direct or indirect interaction between Slam and RhoGEF2.

2.6. *Slam RNA and protein accumulate at the prospective site of invagination*

If Slam mediates the accumulation of RhoGEF2 at the prospective furrow canal, the question arises how Slam itself localizes at these sites. By reexamining the temporal and spatial expression pattern of *slam*, we found that Slam protein is present in low levels before the onset of the strong zygotic expression. These low levels may reflect a maternal contribution. During mitosis 13, Slam staining was found at the metaphase furrows (data not shown) and at the interphase furrows in early cycle 14 (Fig. 7B). We observed an almost exclusive staining at the furrow canal and no staining at the lateral furrow. Besides the staining at the furrow canal, particles of various size basal to the nuclei were stained especially in the first part of cycle 14 (Fig. 7B). Strikingly, we found the same distribution when we stained for *slam* mRNA by fluorescent RNA *in situ* hybridization (Fig. 7A and D). Co-staining of *slam* mRNA and protein showed an extensive match and a stronger protein staining at the furrow canal as compared to the basal particles, especially in later embryos (Fig. 7C and F). These findings are consistent with the previously described slam mRNA localization in blastoderm embryos (Takada et al., 2007). The overlapping RNA and protein distribution may suggest that Slam mRNA is involved in Slam protein localization at the furrow canal.

3. Discussion

RhoGEF2 is an essential regulator of Rho1 activity during many different stages of *Drosophila* development including cellularization (Barrett et al., 1997; Dawes-Hoang et al., 2005; Grosshans et al., 2005; Häcker and Perrimon, 1998; Nikolaidou and Barrett, 2004; Padash Barmchi et al., 2005). However, little has been known about the events and factors that control RhoGEF2 localization and subsequent Rho1 activation at the

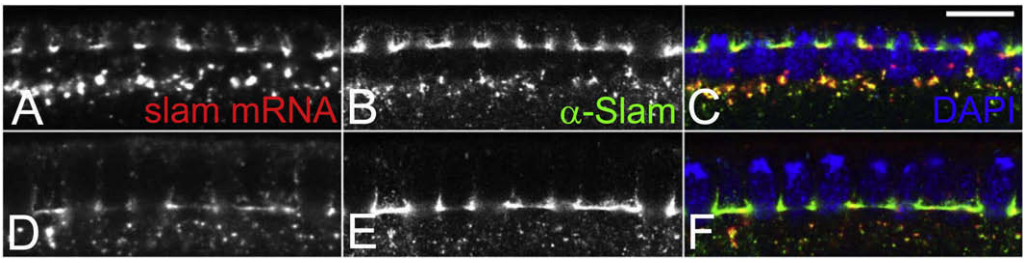

Fig. 7 – Slam mRNA and protein colocalize in basal particles and at the furrow canal. Wildtype embryos were fixed and stained for *slam* mRNA (A and D) and for Slam protein (B and E). (C and F) Merge and DNA stain. Slam mRNA localizes in large basal particles that are most prominent in early cellularization (A). In addition the transcript also localizes to the furrow canal. The slam mRNA signal at the furrow canal decreases in late cellularization and is almost absent at the beginning of gastrulation (D). The slam protein colocalizes with the transcript to a large extent both in the basal particles as well as at the furrow canal (B, C, E and F). Scale bar: 10 μm.

furrow canal. Here we assign a new function to the PDZ domain of RhoGEF2 in being sufficient and required for furrow canal localization. The pattern and the dynamics of furrow canal localization of different PDZ_{RG2} containing constructs are very similar to that of endogenous RhoGEF2 thereby reflecting the behaviour of the full-length protein during cellularization. The domain could be used to effectively target other proteins like RFP, myc or GST to the furrow canal. Thus despite being a multidomain protein, furrow canal localization depends ultimately only on residues that assure the structural integrity of the ligand recognition site of the PDZ domain. It was reported previously that the RhoGEF2 PDZ domain is involved in the subcellular localization of RhoGEF2 during apical constriction of mesodermal cells in gastrulation (Kölsch et al., 2007). It has been suggested that a direct interaction between the PDZ domain and the PDZ binding motive at the C-terminus of the apically localized transmembrane protein T48 is involved in the recruitment of RhoGEF2 to the apical site of the cells. However, it is clear that this interaction is not essential for apical RhoGEF2 localization, since this localization is lost only in *T48/cta* double mutants.

By using immunoprecipitations from staged embryonic extracts we could show that a transgenic $4xPDZ_{RG2}$-myc_6 construct can physically interact with Slam *in vivo*. Of course this does not directly proof that Slam also interacts with full-length endogenous RhoGEF2. Nevertheless we present different arguments that support the assumption that a physical interaction between Slam and RhoGEF2 underlies the observed functional relationship between these two factors in cellularizing embryos. As described above the PDZ domain is the critical element that mediates the localization of RhoGEF2 at the furrow canal where it colocalizes with Slam. We could show that this PDZ domain can form a complex with Slam *in vivo*. *Further in vivo* experiments confirmed that furrow canal localization of RhoGEF2 depends on *slam* in a dosage dependent manner which supports the biochemical findings. Moreover Slam can recruit RhoGEF2 to ectopic sites in embryos as well as in S2 cells and we can observe aspects of the *RhoGEF2* mutant phenotype in *slam* deficient embryos. Overall we think it is reasonable to conclude that there is the possibility of a direct or indirect interaction between Slam and RhoGEF2 during formation of the cellular blastoderm. This interaction would be mediated by the PDZ domain of RhoGEF2. Our data also demonstrate that *slam* acts upstream of *RhoGEF2*.

The molecular function of *slam* has remained unknown, although the essential role of this gene in cellularization is well established (Merrill et al., 1988). It has been proposed that Slam is involved in membrane traffic, since in *slam* mutants the polarized insertion of membrane is disturbed (Lecuit et al., 2002). Here we describe an additional cell biological function of *slam* in being a developmental switch that temporally and spatially controls Rho activity in blastoderm embryos by regulating the subcellular localization of the Rho1 activator RhoGEF2. Thus by proposing the existence of a protein complex containing RhoGEF2 and Slam, we can link physiological and molecular function of Slam.

PDZ domains often interact with the C-termini of transmembrane proteins. There are different classes of PDZ binding motifs that can be classified according to their amino acid composition (Jelen et al., 2003). Although not being a transmembrane but a membrane associated protein (Lecuit et al., 2002), Slam posseses a potential class II PDZ binding motif at its C-terminus. However, this motif seems to be dispensable for the recruitment of RhoGEF2 by Slam to ectopic sites. This is consistent with the fact that a *slam* allele with a mutated C-terminus rescued the cellularization phenotype of *slam* deficient embryos (data not shown). In addition this allele was able to recruit RhoGEF2 to the furrow canal membrane. Furthermore we can observe RhoGEF2 to be still present although with reduced levels at the furrow canal in germline clones of a C-terminally truncated *slam* allele $slam^{waldo1}$.

Besides the interaction between Slam and the PDZ domain of RhoGEF2, we also observed an interaction between Slam and Patj in our co-IPs from staged embryonic extracts. This is consistent with the fact that both proteins almost perfectly colocalize during cellularization at the furrow canal as well as in basal particles (*Supplementary* Fig. S3G and H). Furthermore we also see a functional relation between Slam and Patj, since Patj levels at the furrow canal are reduced in embryos that are zygotically deficient for *slam*. Patj is a conserved protein that contains 4 PDZ domains and was previously reported to be able to interact with Crumbs *in vitro* and *in vivo* during epithelial polarity establishment later in development (Bhat et al., 1999). However, the importance of this interaction remains unclear, since embryos that are maternally and zygotically

mutant for *Patj* have been reported to develop until adulthood without obvious phenotypes (Pielage et al., 2003). This would argue against an essential role of *Patj* during cellularization. As shown by another report, the mutants used in the study mentioned above still expressed a truncated Patj protein that contained the first PDZ domain thus it is likely that residual Patj function was still present (Nam and Choi, 2006). Zygotic *Patj* null mutants, in which the coding sequence of Patj was removed completely, died during second instar larval stage, indicating that Patj is an essential gene. Therefore it would be worth to generate maternal *Patj* null mutants to investigate the role of this protein during cellularization in more detail. Nevertheless the interaction between Patj and Slam seems to depend mainly on the C-terminus of Slam, since in $slam^{waldo1}$ mutants Patj levels at the furrow canal are strongly reduced (*Supplementary* Fig. S3H and K). Thus it is possible that the putative PDZ binding motif at the C-terminus of Slam is important for a direct interaction with one of the PDZ domains of Patj. The Slam Patj interaction also shows that besides controlling RhoGEF2 localization Slam has other independent functions, which could account for the strikingly stronger cellularization phenotype of *slam* mutants compared to the weaker phenotype of *RhoGEF2* deficient embryos.

As mentioned previously *RhoGEF2* also functions in different epithelial invagination processes like salivary gland formation or in the establishment of the epithelium in the wing imaginal disc of *Drosophila* L3 larvae. It appears likely that the subcellular localization of the protein is controlled by genes encoding different receptors that are expressed during different developmental stages in a tissue specific manner like *slam* or *T48* which would allow a very precise temporal and spatial regulation of Rho activity by employing the same ubiquitously expressed activating factor. *RhoGEF2* also has a function in the maternally controlled formation of the metaphase furrows during the cleavage divisions 10–13 of the syncytial blastoderm stage and it was shown that localization of the protein to these furrows depends on maternal components of the recycling endosome (Cao et al., 2008). The start of zygotic *slam* expression at the onset of cellularization thus could assure that sufficient levels of RhoGEF2 and thus Rho activity become associated with the membrane tip during invagination. At the same time the metaphase furrows that have recently been shown to be rather active endocytic membrane domains (Sokac and Wieschaus, 2008a) are transformed into a domain forming the furrow canal, which were reported to be much more inactive and stable (Lecuit and Wieschaus, 2000).

Here we also describe that *slam* transcripts show a new and unique mRNA localization pattern. A significant portion of *slam* mRNA is associated with the furrow canal membrane domain (also described in Takada et al., 2007). Surprisingly the initial processes that ensure a local restriction of Rho activity would be the proper localization of the *slam* RNA/protein particles. The asymmetrical localization of transcripts within a cell often linked with localized translation is an important mechanism for the spatial regulation of gene activity. Apical localization of transcripts during cellularization has been described for a number of genes including *wg*, *run* and *ftz* (Wilkie and Davis, 2001). Here the transcripts are transported to localize to the apical cytoplasm of the cells of the cellular blastoderm. However, little is known about the functional importance of this transcript localization. The localization of *slam* transcripts might also include a basal to apical transport step, since we can observe large basal particles containing *slam* mRNA and protein in cellularizing embryos. It has been reported previously that apical Rho activity during posterior spiracle formation is mediated in part by *RhoGEF64C*. The transcript of this gene does localize to the apical membrane of the epithelial cells which undergo apical constriction and subsequent invagination (Simoes et al., 2006). The mechanisms that ensure the association of transcripts with a specific membrane domain remain to be solved and *slam* would offer a good system to study this question. Future studies will show whether and how the localization of *slam* mRNA is involved in defining the sites for membrane invagination and what other functions are served by *slam* besides initiating Rho signalling.

Taken together, we propose a model for the developmental control of Rho1 signalling at the furrow canal, in that the *slam* RNA–protein particles are targeted to the prospective site of membrane invagination at the onset of cellularization. Slam would have several functions, mainly initiating the formation of the furrow canal as a distinct membrane domain by regulating membrane traffic and at the same time it would recruit and restrict RhoGEF2 and maybe other factors to this domain. After reaching a critical concentration the GEF activity would be activated by a yet unknown mechanism. Rho1 would be converted into its GTP-bound form and downstream targets like Dia or Rho-kinase would be activated. Consistent with this model is our observation that the dose-dependent activity of Slam, both higher or lower than normal levels, directly corresponds to the amount of RhoGEF2 protein and the speed of cellularization as for example shown by the local injection of *slam* RNA.

4. Experimental procedures

4.1. Genetics

OreR flies were used as wildtype controls in Western blots and in some of the immunostainings. Transgenic fly strains were generated by P-element mediated germ line transformation (Rubin and Spradling, 1982) to generate the following constructs: P{w^+, *sqh-myc$_6$-RhoGEF2*}, P{w^+, *sqh-myc$_6$-RhoGEF2 (T1544)*}, P{w^+, *sqh-myc$_6$-RhoGEF2(GAGA)*}, P{w^+, *UAS-GFP-Slam*}, P{w^+, *UAS-RFP-RhoGEF2*}, P{w^+, *UAS-4xPDZ$_{RG2}$-RFP*} and P{w^+, *UAS-4xPDZ$_{RG2}$-myc$_6$*}. Germline expression of the pUASp constructs was driven by P{w^+, *tub-Gal4-VP16*}67 (Chr. II) or P{w$^+$, *tub-Gal4-VP16*}15 (Chr. III). Expression of P{w^+, *UAS-Slam-HA*} (Lecuit et al., 2002) was driven by using driver line P{*prd-Gal4*, w^+}/*TM3, Sb* (Bloomington Stock Center).

Df(2L)BSC5/SM6a (=$slam^{Def}$) flies were obtained from the Bloomington Stock Center and used to generate zygotic *slam* mutants. FRT^{2R} G13 *RhoGEF2* $^{l(2)04291}$/CyO and $slam^{35.16}$ Frt^{2L}/CyO (=$slam^{waldo1}$) were used to generate germline clones by the autosomal FLP/FRT technique (Chou and Perrimon, 1996). For scoring the rescue activity of different myc-tagged *RhoGEF2* alleles a third chromosomal insertion of the respective construct was crossed into the $RhoGEF2^{l(2)04291}$ background to generate for example females of genotype: *w*; FRT^{2R} G13

RhoGEF2$^{l(2)04291}$*/CyO*; P{*w*$^{+}$, *sqh-myc*$_6$*-RhoGEF2*} which were then used to generate germline clones. *RhoGEF2*$^{l(2)04291}$ was reported to lack the transcript (Häcker and Perrimon, 1998).

4.2. Histology

Embryos were fixed either in 4% formaldehyde in PBS or by heat treatment (for RhoGEF2, Nrt and myc-RhoGEF2 stainings) as previously described (Grosshans et al., 2005). S2 cells were fixed for 10 min in 4% formaldehyde in PBS, permeabilized in 0.5% Triton X100 in PBS for 30 s, blocked with 5% BSA in PBT (PBS + 0.1% Tween20) for 15 min and then incubated with the primary antibody in PBT for 1 h. After washing with PBT and incubation with the secondary antibody for 1 h cells were stained with DAPI for 3 min, washed again and finally mounted in Aqua Polymount (Polysciences). Fluorescence RNA *in situ* hybridization was performed according to (Tautz and Pfeifle, 1989). In brief, after the post-hybridization washes, embryos were incubated twice with PBT + 1% BSA for 20 min each at RT and then incubated for 2 h with α-DIG antibody coupled to peroxidase. After that embryos were washed 3× for 1 min and 4× for 15 min with PBT. Staining reaction was started by adding 200 μl of reaction solution (TSA-Cy3 diluted 1:200 in reaction buffer, PerkinElmer) to the embryos for 5–10 min. Embryos were washed 3× with PBT and then used for subsequent antibody co-staining.

The following antibodies were used: Primary antibodies: rabbit-α-RhoGEF2 (Grosshans et al., 2005), guinea pig-α-Slam, rabbit-α-Slam (Brandt et al., 2006), mouse-α-Dlg (Hybridoma Center), mouse-α-myc-9E10 (Roche), mouse-α-Nrt (Hybridoma Center), rabbit-α-Patj (kindly provided by H. Bellen, described in Bhat et al., 1999), mouse-α-Myo (gift from B. Mechler), rabbit-α-Dia (Grosshans et al., 2005), rabbit-α-GFP (Torrey Pines Biolabs), mouse-α-HA (Babco), mouse-α-Rho1 (Magie et al., 2002) and rat-α-Yrt (gift from U. Tepass, described in Laprise et al., 2006), secondary antibodies: Alexa-coupled goat-anti-mouse, goat-anti-rabbit and goat-anti-guineapig (Invitrogen), POD coupled α-Digoxygenin Fab-fragments (Roche). F-actin was stained using Alexa-coupled phalloidin (Invitrogen) and DNA was stained using DAPI.

4.3. Microinjections

Embryos were injected as previously described (Grosshans et al., 2005). The mRNA constructs were injected at concentrations of about 0.5–2 μg/μl. Slam dsRNA was injected at the posterior pole at a concentration of 1 μg/μl.

4.4. Cell culture

Drosophila S2 cells were kept in Schneiders *Drosophila* medium (Gibco/Invitrogen) supplemented with 10% fetal bovine serum (Gibco/Invitrogen) at 25 °C. Cells were transiently transfected either with pCaSpeR-sqh-myc$_6$-RhoGEF2 or with pMT-GFP-Slam and pCaSpeR-sqh-myc$_6$-RhoGEF2 using the Qiagen Effectene Transfection Reagent (Qiagen). After 18–24 h the reagent was removed and cells were seeded on uncoated cover slips. GFP-Slam expression was induced by addition of 0.5 mM $CuSO_4$ to the medium. Sixteen hours later cells were fixed and used for immunostaining.

4.5. Imaging

A Zeiss Axiovert 200 M PerkinElmer Ultra-View Spinning Disc konfocal microscope (63× NA 1.4 oil Apochromat and 100× NA 1.4 oil) was used for timelapse recordings of embryos expressing RFP fusion proteins, as well as for imaging of fixed and immunostained S2 cells (flatfield capture mode). Fluorescence was excited using 488 and 546 nm laser light. For live imaging z-stacks of 5–10 images covering a distance of 5–10 μm were recorded. Appropriate layers were subsequently selected for further analysis. Fluorescent images of fixed and immunostained embryos were recorded with a Leica confocal microscope (DMIRE2, HCX PL APO 63× NA 1.4 oil, laser at 405, 488, 568, 633 nm). Images were processed with ImageJ and Adobe Photoshop.

4.6. Immunoprecipitation

Embryonic extracts were prepared by lysing 100 mg of 2–3 h old embryos in RIPA buffer (10 mM Tris/HCl pH 7.5, 150 mM NaCl, 0.1% SDS, 1% Triton X 100, 1% Deoxycholate, 5 mM EDTA, 2 mM PMSF, 1× protease inhibitor cocktail complete Mini EDTA-free, Roche) in a Dounce homogenizer. The suspension was centrifuged for 15 min at 20,000*g* to remove debris. The supernatant was immediately used for IP-experiments. Guinea pig-α-Slam antibody (serum) or preimmune serum was coupled to Protein-A-Sepharose beads (GE Healthcare) in PBT for 1 h at 4 °C. Beads were washed five times with PBT before freshly prepared embryonic extract was added. The samples were incubated on a rotator for 60 min at 4 °C. A sample was taken from the supernatant (unbound fraction). Beads were then washed 3 times with dilution buffer (10 mM Tris/HCl pH 7.5, 150 mM NaCl, 0.5 mM EDTA, 1 mM freshly added PMSF, 1× protease inhibitors) and 2× with washing buffer (10 mM Tris/HCl pH 7.5, 300 mM NaCl, 0.5 mM EDTA, 1 mM PMSF, 1× protease inhibitors). Bound proteins were eluted in 50 μl laemmli buffer and analyzed using SDS–PAGE and subsequent Western blotting.

4.7. Molecular genetics

A detailed list of all constructs used in this study is included in the Supplementary data. The dsRNA probe directed against *slam* was generated as previously described (Lecuit et al., 2002) using the T7 MEGAscript High Yield Transcription Kit (Applied Biosystems). Capped transcripts were synthesized using the SP6 mMESSAGE mMACHINE high yield capped RNA transcription kit (Applied Biosystems).

Acknowledgments

We would like to thank U. Tepass, A. Müller, D. Görlich, M. Rupp, E. Wieschaus, T. Lecuit, U. Häcker, D. Kiehart, R. Tsien, H. Bellen, B. Mechler and C. Hunter for sharing fly stocks and reagents. This work was supported by the Deutsche Forschungsgemeinschaft.

Appendix A. Supplementary data

Supplementary data associated with this article can be found, in the online version, at doi:10.1016/j.mod.2010.01.001.

REFERENCES

Afshar, K., Stuart, B., Wasserman, S.A., 2000. Functional analysis of the Drosophila Diaphanous FH protein in early embryonic development. Development 127, 1887–1897.

Barrett, K., Leptin, M., Settleman, J., 1997. The Rho GTPase and a putative RhoGEF mediate a signaling pathway for the cell shape changes in Drosophila gastrulation. Cell 91, 905–915.

Bement, W.M., Benink, H.A., von Dassow, G., 2005. A microtubule-dependent zone of active RhoA during cleavage plane specification. J. Cell Biol. 170, 91–101.

Bhat, M.A., Izaddoost, S., Lu, Y., Cho, K.O., Choi, K.W., Bellen, H.J., 1999. Discs lost, a novel multi-PDZ domain protein, establishes and maintains epithelial polarity. Cell 96, 833–845.

Brandt, A., Papagiannouli, F., Wagner, N., Wilsch-Bräuninger, M., Braun, M., Furlong, E.E., Loserth, S., Wenzl, C., Pilot, F., Vogt, N., et al, 2006. Developmental control of nuclear size and shape by Kugelkern and Kurzkern. Curr. Biol. 16, 543–552.

Bustelo, X.R., Sauzeau, V., Berenjeno, I.M., 2007. GTP-binding proteins of the Rho/Rac family: regulation, effectors and functions in vivo. Bioessays 29, 356–370.

Cao, J., Albertson, R., Riggs, B., Field, C.M., Sullivan, W., 2008. Nuf, a Rab11 effector, maintains cytokinetic furrow integrity by promoting local actin polymerization. J. Cell Biol. 182, 301–313.

Chou, T.B., Perrimon, N., 1996. The autosomal FLP-DFS technique for generating germline mosaics in *Drosophila melanogaster*. Genetics 144, 1673–1679.

Crawford, J.M., Harden, N., Leung, T., Lim, L., Kiehart, D.P., 1998. Cellularization in *Drosophila melanogaster* is disrupted by the inhibition of rho activity and the activation of Cdc42 function. Dev. Biol. 204, 151–164.

D'Avino, P.P., Savoian, M.S., Glover, D.M., 2005. Cleavage furrow formation and ingression during animal cytokinesis: a microtubule legacy. J. Cell Sci. 118, 1549–1558.

Dawes-Hoang, R.E., Parmar, K.M., Christiansen, A.E., Phelps, C.B., Brand, A.H., Wieschaus, E.F., 2005. Folded gastrulation, cell shape change and the control of myosin localization. Development 132, 4165–4178.

Grosshans, J., Wenzl, C., Herz, H.M., Bartoszewski, S., Schnorrer, F., Vogt, N., Schwarz, H., Müller, H.A., 2005. RhoGEF2 and the formin Dia control the formation of the furrow canal by directed actin assembly during Drosophila cellularisation. Development 132, 1009–1020.

Häcker, U., Perrimon, N., 1998. DRhoGEF2 encodes a member of the Dbl family of oncogenes and controls cell shape changes during gastrulation in Drosophila. Genes Dev. 12, 274–284.

Jaffe, A.B., Hall, A., 2005. Rho GTPases: biochemistry and biology. Annu. Rev. Cell Dev. Biol. 21, 247–269.

Jelen, F., Oleksy, A., Smietana, K., Otlewski, J., 2003. PDZ domains – common players in the cell signaling. Acta Biochim. Pol. 50, 985–1017.

Kamijo, K., Ohara, N., Abe, M., Uchimura, T., Hosoya, H., Lee, J.S., Miki, T., 2006. Dissecting the role of Rho-mediated signaling in contractile ring formation. Mol. Biol. Cell 17, 43–55.

Kölsch, V., Seher, T., Fernandez-Ballester, G.J., Serrano, L., Leptin, M., 2007. Control of Drosophila gastrulation by apical localization of adherens junctions and RhoGEF2. Science 315, 384–386.

Laprise, P., Beronja, S., Silva-Gagliardi, N.F., Pellikka, M., Jensen, A.M., McGlade, C.J., Tepass, U., 2006. The FERM protein Yurt is a negative regulatory component of the Crumbs complex that controls epithelial polarity and apical membrane size. Dev. Cell 11, 363–374.

Lecuit, T., Samanta, R., Wieschaus, E., 2002. Slam encodes a developmental regulator of polarized membrane growth during cleavage of the Drosophila embryo. Dev. Cell 2, 425–436.

Lecuit, T., Wieschaus, E., 2000. Polarized insertion of new membrane from a cytoplasmic reservoir during cleavage of the Drosophila embryo. J. Cell Biol. 150, 849–860.

Lee, J.S., Kamijo, K., Ohara, N., Kitamura, T., Miki, T., 2004. MgcRacGAP regulates cortical activity through RhoA during cytokinesis. Exp. Cell Res. 293, 275–282.

Longhurst, D.M., Watanabe, M., Rothstein, J.D., Jackson, M., 2006. Interaction of PDZRhoGEF with microtubule-associated protein 1 light chains: link between microtubules, actin cytoskeleton, and neuronal polarity. J. Biol. Chem. 281, 12030–12040.

Magie, C.R., Pinto-Santini, D., Parkhurst, S.M., 2002. Rho1 interacts with p120ctn and alpha-catenin, and regulates cadherin-based adherens junction components in Drosophila. Development 129, 3771–3782.

Mazumdar, A., Mazumdar, M., 2002. How one becomes many: blastoderm cellularization in *Drosophila melanogaster*. Bioessays 24, 1012–1022.

Merrill, P.T., Sweeton, D., Wieschaus, E., 1988. Requirements for autosomal gene activity during precellular stages of *Drosophila melanogaster*. Development 104, 495–509.

Mulinari, S., Barmchi, M.P., Häcker, U., 2008. DRhoGEF2 and diaphanous regulate contractile force during segmental groove morphogenesis in the Drosophila embryo. Mol. Biol. Cell 19, 1883–1892.

Nakaya, Y., Sukowati, E.W., Wu, Y., Sheng, G., 2008. RhoA and microtubule dynamics control cell-basement membrane interaction in EMT during gastrulation. Nat. Cell Biol. 10, 765–775.

Nam, S.C., Choi, K.W., 2006. Domain-specific early and late function of Dpatj in Drosophila photoreceptor cells. Dev. Dyn. 235, 1501–1507.

Nikolaidou, K.K., Barrett, K., 2004. A Rho GTPase signaling pathway is used reiteratively in epithelial folding and potentially selects the outcome of Rho activation. Curr. Biol. 14, 1822–1826.

Padash Barmchi, M., Rogers, S., Häcker, U., 2005. DRhoGEF2 regulates actin organization and contractility in the Drosophila blastoderm embryo. J. Cell Biol. 168, 575–585.

Pielage, J., Stork, T., Bunse, I., Klämbt, C., 2003. The Drosophila cell survival gene discs lost encodes a cytoplasmic Codanin-1-like protein, not a homolog of tight junction PDZ protein Patj. Dev. Cell 5, 841–851.

Prokopenko, S.N., Brumby, A., O'Keefe, L., Prior, L., He, Y., Saint, R., Bellen, H.J., 1999. A putative exchange factor for Rho1 GTPase is required for initiation of cytokinesis in Drosophila. Genes Dev. 13, 2301–2314.

Rogers, S.L., Wiedemann, U., Häcker, U., Turck, C., Vale, R.D., 2004. Drosophila RhoGEF2 associates with microtubule plus ends in an EB1-dependent manner. Curr. Biol. 14, 1827–1833.

Rubin, G.M., Spradling, A.C., 1982. Genetic transformation of Drosophila with transposable element vectors. Science 218, 348–353.

Schejter, E.D., Wieschaus, E., 1993. Functional elements of the cytoskeleton in the early Drosophila embryo. Annu. Rev. Cell Biol. 9, 67–99.

Schmidt, A., Hall, A., 2002a. Guanine nucleotide exchange factors for Rho GTPases: turning on the switch. Genes Dev. 16, 1587–1609.

Schmidt, A., Hall, A., 2002b. The Rho exchange factor Net1 is regulated by nuclear sequestration. J. Biol. Chem. 277, 14581–14588.

Shaw, R.M., Fay, A.J., Puthenveedu, M.A., von Zastrow, M., Jan, Y.N., Jan, L.Y., 2007. Microtubule plus-end-tracking proteins target gap junctions directly from the cell interior to adherens junctions. Cell 128, 547–560.

Simoes, S., Denholm, B., Azevedo, D., Sotillos, S., Martin, P., Skaer, H., Hombria, J.C., Jacinto, A., 2006. Compartmentalisation of Rho regulators directs cell invagination during tissue morphogenesis. Development 133, 4257–4267.

Sokac, A.M., Wieschaus, E., 2008a. Local actin-dependent endocytosis is zygotically controlled to initiate Drosophila cellularization. Dev. Cell 14, 775–786.

Sokac, A.M., Wieschaus, E., 2008b. Zygotically controlled F-actin establishes cortical compartments to stabilize furrows during Drosophila cellularization. J. Cell Sci. 121, 1815–1824.

Somers, W.G., Saint, R., 2003. A RhoGEF and Rho family GTPase-activating protein complex links the contractile ring to cortical microtubules at the onset of cytokinesis. Dev. Cell 4, 29–39.

Stein, J.A., Broihier, H.T., Moore, L.A., Lehmann, R., 2002. Slow as molasses is required for polarized membrane growth and germ cell migration in Drosophila. Development 129, 3925–3934.

Takada, S., Kwak, S., Koppetsch, B.S., Theurkauf, W.E., 2007. Grp (chk1) replication-checkpoint mutations and DNA damage trigger a Chk2-dependent block at the Drosophila midblastula transition. Development 134, 1737–1744.

Tatsumoto, T., Xie, X., Blumenthal, R., Okamoto, I., Miki, T., 1999. Human ECT2 is an exchange factor for Rho GTPases, phosphorylated in G2/M phases, and involved in cytokinesis. J. Cell Biol. 147, 921–928.

Tautz, D., Pfeifle, C., 1989. A non-radioactive in situ hybridization method for the localization of specific RNAs in Drosophila embryos reveals translational control of the segmentation gene hunchback. Chromosoma 98, 81–85.

Tcherkezian, J., Lamarche-Vane, N., 2007. Current knowledge of the large RhoGAP family of proteins. Biol. Cell 99, 67–86.

Warn, R.M., Magrath, R., 1983. F-actin distribution during the cellularization of the Drosophila embryo visualized with FL-phalloidin. Exp. Cell Res. 143, 103–114.

Wilkie, G.S., Davis, I., 2001. Drosophila wingless and pair-rule transcripts localize apically by dynein-mediated transport of RNA particles. Cell 105, 209–219.

Supplement

Supplementary Figures

Supplementary Figure S1:

4xPDZ$_{RG2}$-RFP shows a similar localization behaviour as RFP-RhoGEF2

Cellularization was recorded in embryos expressing 4xPDZ$_{RG2}$-RFP or RFP-RhoGEF2. A-G: pictures from a timelapse series of embryos expressing 4xPDZ$_{RG2}$-RFP (taken at a representative z-position). The construct localizes to centrosomes and to the mitotic spindle during interphase 13 and mitosis 13. At beginning of cellularization in interphase 14 the protein is enriched around centrosomes and starts accumulating at the presumptive membrane invagination site slightly later where it then associates with the furrow canals (D). The furrow canal association is strongly disrupted in embryos treated with slam RNAi (E-G). Whereas spindle and pericentrosomal localization is not affected (E and F), 4xPDZ$_{RG2}$-RFP does not accumulate at the furrow canal (G).

Similar as the 4xPDZ$_{RG2}$-RFP construct the full length protein shows a similar localization behaviour (H-J). It can be detected at centrosomes (white arrows in H) and mitotic spindles (I) and at the furrow canals (J). Pictures were taken from three different embryos. Expression of RFP-RhoGEF2 causes variable dominant effects that lead to disruptions in mitosis and cellularization (arrow in J). Scalebars: 10 µm.

Supplementary Figure S2:

Localization of the lateral marker Dlg in *slam* embryos

C-H: *slam* embryos were stained together with their heterozygous siblings for Slam (C and F) and Dlg (D and G), merge in E and H. In contrast to Slam, the levels of Dlg at the lateral membrane were similar to wildtype. A, B, I, J: Plot profiles of the corresponding signals from C, D, F, G. Intensity profiles were plotted along the indicated yellow freehand lines. Scale bar: 10 µm.

Supplementary Figure S3:

Furrow canal localization of Patj strongly depends on the C-terminal part of Slam

WT embryos and embryos from *slam^{waldo1}* germline clones were fixed and stained together for Slam (A, D, G and J), RhoGEF2 (B, E), Patj (H, K) and DAPI (overlay in C, F, I and L). *slam^{waldo1}* encodes a C-terminally truncated protein of 698 amino acids (Stein et al., 2002).

This protein does localize to the furrow canal but the levels are reduced compared to the staining of wildtype embryos (A and D, G and J). Moreover there is a diffuse apical staining (D). The levels of RhoGEF2 at the furrow canal are also reduced and in contrast to wildtype an apical enrichment of the protein can be observed (B and E). Furrow canal localization of Patj is strongly reduced in *slam* mutants (H and K). The difference in Slam staining between D and J results from different fixation methods. Embryos in A-F were heatfixed, embryos in G-L were fixed using formaldehyde. Scalebars: 10 µm.

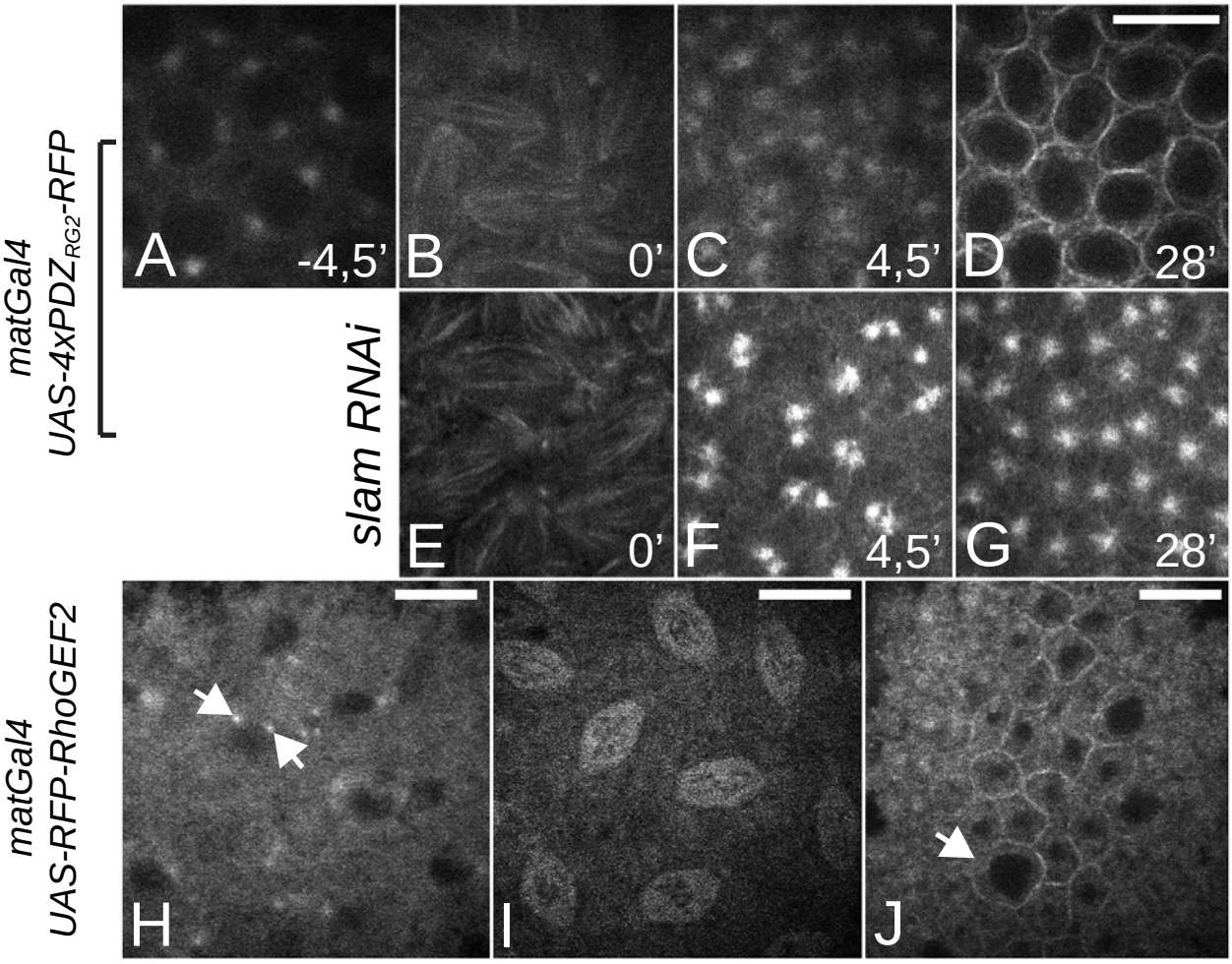

Figure S1
Wenzl *et al.*

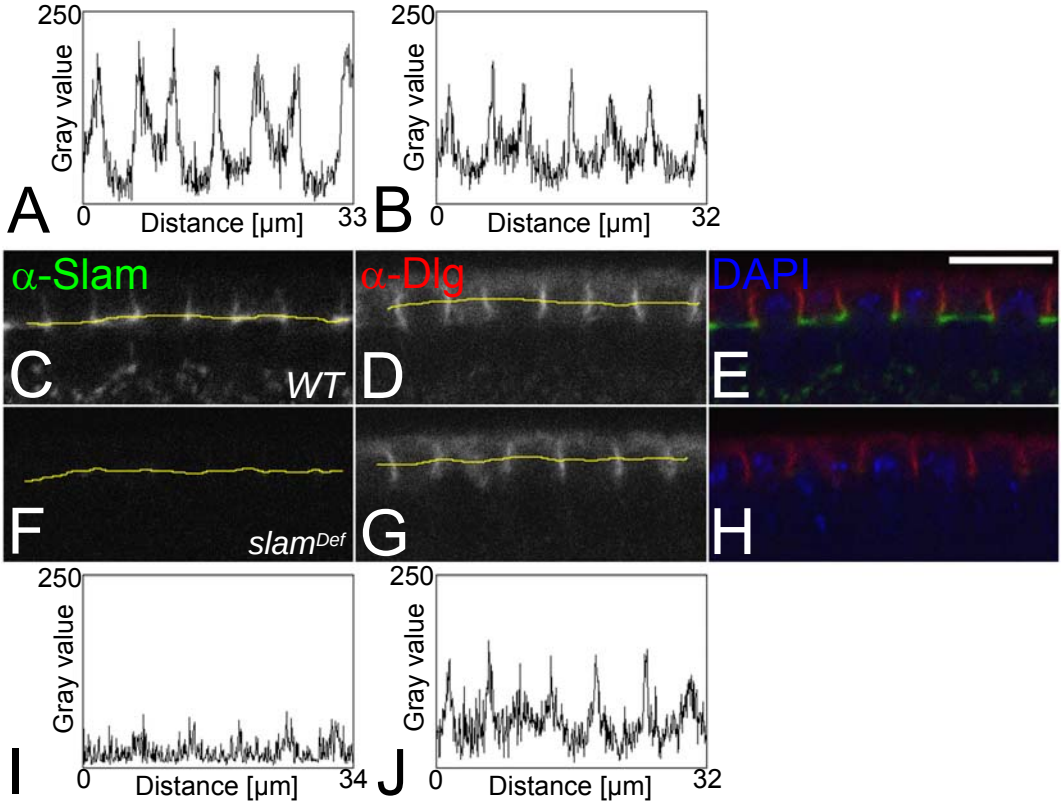

Figure S2
Wenzl *et al.*

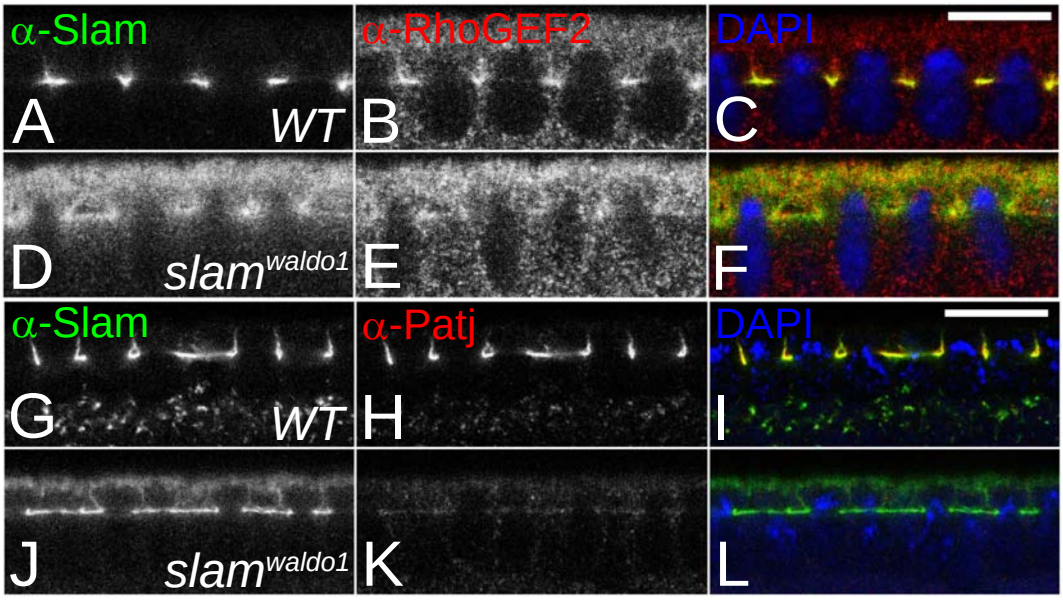

Figure S3
Wenzl *et al.*

Supplementary Material and Methods:

name of construct	oligos	cloning
pCS2MT-RhoGEF2		see text description
pCS2MT-RhoGEF2-I	CW5a, CW5b	cloned as EcoRI/XhoI fragment in pCS2MT (gift from M.Rupp, Munich)
pCS2MT-RhoGEF2-IA	CW5a, CW5c	cloned as EcoRI/XhoI fragment in pCS2MT
pCS2MT-RhoGEF2-IB	CW5e, CW5b	cloned as EcoRI/XhoI fragment in pCS2MT
pCS2MT-RhoGEF2-IB(GAGA)	CW32a, CW32b	see text description
pCS2MT-RhoGEF2-II	CW6a, CW6b	cloned as EcoRI/XhoI fragment in pCS2MT
pCS2MT-RhoGEF2-III	CW7a, CW7b	cloned as XbaI/XbaI fragment in pCS2MT
pCS2MT-RhoGEF2-IV	CW8a, CW8b	cloned as EcoRI/XhoI fragment in pCS2MT
pCS2MT-4xPDZ$_{RG2}$	CW21a, CW21b CW22a, CW22b	see text description
pCS2MT-GST-2xPDZ$_{RG2}$	CW28a, CW28b	see text description
pUASP-4xPDZ$_{RG2}$-RFP	CW29a, CW29b	see text description
pUASP-4xPDZ$_{RG2}$-myc$_6$		see text description
pUASP-RFP-RhoGEF2	CW37a, CW37b CW37c, CW17b	see text description
pCaSpeR_sqh -myc$_6$+RhoGEF2	CW26c, CW17b CW27a, CW27b	see text description
pCaSpeR_sqh-myc$_6$+RhoGEF2(GAGA)		see text description
pCaSpeR_sqh-myc$_6$+RhoGEF2(T1544A)		see text description
pCS2-Slam		see text description
pCS2MT-Slam4	JG263, JG107	cloned as EcoRI/Xba fragment into pCS2MT
pCS2MT-Slam	SY20, SY21	cloned as EcoRI/XbaI fragment into pCS2MT (using pCS2-Slam as template)
pCS2MT-SlamCX	CW81a, CW81b	see text description
pMT-GFP-Slam	CW43a, CW43b	see text description

Table S1 - list of constructs

The indicated DNA sequences were amplified by PCR using Vent-Polymerase (New England Biolabs, USA), digested by appropriate restriction enzymes and cloned into the indicated vectors. Site directed mutagenesis was performed using inverse PCR with Pfu-Polymerase (Stratagene, USA) and subsequent DpnI digest of the template. A description for all constructs used in this study including all employed oligos is given in table S1 or in the description below.

pCS2MT-RhoGEF2:

A 7,34 kb SmaI/XbaI fragment from pCS2-RhoGEF2 was cloned in pCS2MT-RhoGEF2-I that had been digested with SmaI/XbaI. pCS2-RhoGEF2 was cloned by EcoRI/XhoI digestion of pOT2-RhoGEF2 (RhoGEF2 EST SD04476) and subsequent 4 point ligation of the resulting 3 fragments into pCS2.

pCS2MT-RhoGEF2-IB-GAGA:

Site directed mutagenesis was performed by inverse PCR using oligos CW32a, CW32b and vector pCS2MT-RhoGEF2-IB as template. After mutagenesis the EcoRI/XhoI fragment containing the mutations was transfered into pCS2MT.

pCS2MT-4xPDZ$_{RG2}$:

The PDZ domain of RhoGEF2 (aa 241-349) was PCR amplified using oligos CW22a (introducing a ClaI site) and CW22b (ClaI) and cloned as ClaI/ClaI fragment into pCS2MT. Clones with correctly oriented double insertions were isolated to get the intermediate construct pCS2MT-2xPDZ$_{RG2}$. The same PCR fragment was cloned into the non-methylated ClaI site at the 3' end of the insert in pCS2MT-2xPDZ$_{RG2}$ to create pCS2MT-3xPDZ$_{RG2}$. Finally a fourth copy of the PDZ domain was PCR amplified by using CW21a (BamHI+ATG) and CW21b (BamHI) and cloned into the BamHI site of pCS2MT-3xPDZ$_{RG2}$.

pCS2MT-GST-2xPDZ$_{RG2}$:

The GST ORF was PCR amplified using oligos CW28a (BamHI), CW28b (BamHI) and pGEX60H as template. The fragment was cloned into the BamHI site of pCS2MT-2xPDZ$_{RG2}$.

pUASP-4xPDZ$_{RG2}$-RFP:

The coding sequence of mRFP was amplified using CW29a (ClaI), CW29b (EcoRI) and pRSETB-mRFP1 as template (gift from R.Tsien described in Campbell et al., 2002). The PCR fragment was cloned into ClaI/EcoRI digested pCS2MT-4xPDZ$_{RG2}$ thereby replacing the C-terminal 6xmyc tag by RFP. After that a 2091bp HindIII/EcoRI fragment was excised and cloned into pBluescript II SK(+) (pBSIISK, Stratagene). From the resulting vector pBSIISK-4xPDZ$_{RG2}$-RFP a 2153 bp KpnI/XbaI fragment was excised and cloned into pUASP (Rørth, 1998).

pUASP-4xPDZ$_{RG2}$-myc$_6$:

A HindIII/EcoRI fragment containing the sequence encoding 4xPDZ$_{RG2}$-myc$_6$ was excized from pCS2MT-4xPDZ$_{RG2}$ and cloned into equally digested pBluescript KS(+). This vector was digested with EcoRI, blunted and subsequently digested with KpnI. The resulting fragment was cloned into pUASP that had been digested with NotI, blunted and subsequently digested with KpnI. Due to the cloning procedure the C-terminus of the 4xPDZ$_{RG2}$-myc$_6$ fusion protein encoded by pUASP-4xPDZ$_{RG2}$-myc$_6$ is slightly different from the one encoded by pCS2MT-4xPDZ$_{RG2}$.

pUASP-RFP-RhoGEF2:

The ORF of mRFP was amplified using CW37a (KpnI), CW37b (HindIII) and pRSETB-mRFP1 as template and cloned into pBSKS to generate pBSKS-RFP. The N-terminal part of RhoGEF2 was amplified using CW37c (HindIII), CW17b and pCS2-RhoGEF2 as template. After digestion with HindIII und SmaI (internal site) the PCR fragment was cloned into pBSKS-RFP. A 7,34 kb SmaI/XbaI Fragment from pCS2-RhoGEF2 was excised and cloned into pBSKS-RFP-RG2(N-term). From the resulting construct pBSKS-RFP-RhoGEF2 a 8,7 kb KpnI/XbaI fragment containing the RFP-RhoGEF2 sequence was excised and cloned into pUASP.

pCaSpeR-sqh-myc$_6$-RhoGEF2:

Cloning of this construct was based on vector sGMCA (gift from D. Kiehart, Kiehart et al., 2000). This vector is a modified pCaSpeR which contains promoter and 3'UTR of the *spaghetti sqash* (*sqh*) gene. The N-terminal part of RhoGEF2 including the 6xmyc epitop was amplified using CW 26c (NgoMIV), CW 17b and pCS2MT+RhoGEF2-I as template. The PCR product was digested with NgoMVI and SmaI (internal site) and cloned into NgoMIV/SmaI digested pBSIISK to create intermediate pBSIISK-myc$_6$-RhoGEF2_N-term. A 7,3 kb SmaI/XbaI fragment from pCS2-RhoGEF2 was cloned into pBSIISK-myc$_6$-RhoGEF2_N-term to create pBSIISK-myc$_6$-RhoGEF2. The 3'-UTR of *sqh* was amplified using CW27a (SpeI), CW27b and sGMCA as template. The PCR fragment was digested with SpeI/XbaI (internal site) and cloned into the XbaI site of pBSIISK-myc$_6$-RhoGEF2 to create pBSIISK-myc$_6$-RhoGEF2-3'UTRsqh. From this vector a 5,3 kb NgoMIV/XbaI fragment and a 3,4 kb NgoMIV/NgoMIV were excised and consecutively cloned into NgoMIV/XbaI digested sGMCA.

pCaSpeR-sqh-myc$_6$-RhoGEF2-GAGA

To introduce the two point mutations in the PDZ domain a 1,2 kb SmaI/AvrII fragment was excised from pBSIISK-myc$_6$-RhoGEF2-3'UTRsqh and replaced by the respective fragment excised from pCS2MT-RhoGEF2-IB-GAGA. The cloning into the sGMCA backbone was done as decribed for pCaSpeR_sqh -myc$_6$+RhoGEF2.

pCaSpeR-sqh-myc$_6$-RhoGEF2-T1544A:

pCaSpeR+sqh+myc6+RhoGEF2 was digested with AvrII/PmeI and the excised 3,67 kb fragment was replaced by the respective fragment excised from pCS2-RhoGEF2-T1544A (pCS2-RhoGEF2-T1544A was generated by inserting a 0,8 kb EcoRI/XhoI fragment from pGEX4T-GST-GEF2-T1544A (Grosshans et al., 2005) into pCS2 and subsequent addition of a 4,6 kb EcoRI/EcoRI and a 3 kb XhoI/XhoI fragment).

pCS2-Slam:

pOT2-Slam (Slam EST LD22808) was EcoRI/XhoI digested and the resulting two fragments were consecutively cloned into pCS2.

pCS2MT-SlamCX:

A 519 bp SacII/SacII fragment was excised from pCS2MT-Slam and replaced by the respective fragment from pCS2MT-Slam4-CX. For pCS2MT-Slam4-CX site directed mutagenesis was performed by inverse PCR using oligos CW81a, CW81b and vector pCS2MT-Slam4 as template. After mutagenesis the mutated EcoRI/XbaI fragment was excised and cloned into equally digested pCS2MT.

pMT-GFPSlam:

The coding region of GFP was PCR amplified using CW43a (KpnI), CW43b (EcoRI) and GMCA as template and cloned as KpnI/EcoRI fragment into pMT-V5-His-C (Invitrogen) to generate pMT-GFP. An EcoRI/NotI fragment was excised from pCS2-Slam9. The NotI site was blunted and the fragment was cloned into EcoRI/EcoRV digested pMT-GFP. pCS2-Slam9 was cloned by amplifying the Slam ORF using SY24 (EcoRI), SY21 and pCS2-Slam as template. The PCR fragment was digested with EcoRI and XbaI (internal site) and cloned into pCS2MT.

list of oligos:

SY20 : GCG GAA TTC AAT GCC AGA AAG CCA CAG TTA C
SY21 : GTA ATA CGA CTC ACT ATA GTT CTA G
SY24 : GAA GAG GAC TTG AAT TCA TAT GCC AGA AAG CCA CAG
JG107: GTA ATA CGA CTC ACT ATA G
JG261: GCG AGA ATT CCG AGT CCA AGA AGG AGA CAC AAG
JG262: ACC TCT CGA GTT ATC CGC TGA GGA AGG CAA ACA G
JG263: TCT AGA ATT CGC GGG AGT TCT TCG CCA ATG
CW5a : GCA GAA TTC AAT GAC CCA TCA ATC AAA AAA CG
CW5b : ATC CTC GAG TTA AGG CGG TAG CGG TGG TGG
CW5c : TAC GCT CGA GTT AGT CCA CCG GCT GTG GCC C
CW5e : TGC AGA ATT CCA ACG GCA GCA TAA TGG GCG
CW6a : GCA GAA TTC ACG CTT GCC TGG CAT GAT G
CW6b : ATC CTC GAG TTA TGG ATC AGA GGT CTT GCG G
CW7a : GCA TCT AGA AAG CTT GTC GTC GCG TCC C
CW7b : ACC TCT AGA TTA CTT CTG AAT GGG TTC GCC
CW8a : GCA GAA TTC ATA TTC GGC GAA TGG GAC GG
CW8b : ATC CTC GAG TTA TTC CTC ATC CTC AGT GCT AG
CW17b: GCC TGC AAT CTC CGC TGC
CW22a: TAG CCG ATC GAT CGC CGA GTA CGC CAA GCC
CW22b: GCA AGT ATC GAT GAA TGG GTG TCG AGG GCG
CW26c: CAG TCA GCC GGC CTT GTT CTT TTT GCA GGA TCC C
CW27a: TGC ATA CTA GTC TAG CAG TCG ATT CAC TAG CCA GC
CW27b: GGT GGT CCC GTC GGC AAG AG
CW28a: TGC AGG ATC CAT GTC CCC TAT ACT AGG TTA TTG G
CW28b: ACC TGG ATC CAT CCG ATT TTG GAG GAT GG
CW29a: TAG CCG ATC GAT TAG CCT CCT CCG AGG ACG TCA TC
CW29b: CAG TGA ATT CTT AGG CGC CGG TGG AGT GGC
CW32a: AAA GAT AGC AAC GGA GCC GGG GCG AAG GTT TCC GGA GAT
CW32b: ATC TCC GGA AAC CTT CGC CCC GGC TCC GTT GCT ATC TTT
CW37a: TGC GGT ACC ATG GCC TCC TCC GAG GAC
CW37b: ACT AAG CTT GGC GCC GGT GGA GTG GCG
CW37c: GTC TAA GCT TAT GAC CCA TCA ATC AAA AAA CG
CW43a: TGC GGT ACC ATG GTG AGC AAG GGC GAG G

CW43b: CTA GAA TTC GGT ACA GCT CGT CCA TGC CG

CW81a: ATG GAC CGG AGG GCC GCA GAG GCC TGA GCG ATG GTG CTA

CW81b: TAG CAC CAT CGC TCA GGC CTC TGC GGC CCT CCG GTC CAT